



Nuclear Materials Authority
P.O.Box 530 Maadi, Cairo, Egypt

DOAJ DIRECTORY OF
OPEN ACCESS
JOURNALS

ISSN 2314-5609
Nuclear Sciences Scientific Journal
9, 79- 102
2020
<http://www.ssnma.com>

ORIGIN OF Mn-Fe ORE BEARING RADIOACTIVE MINERALS AT UM BOGMA AREA, SOUTHWESTERN SINAI, EGYPT

OSAMA R. SALLAM

Nuclear Materials Authority, P.O. Box – 530 Maadi, Cairo, Egypt

ABSTRACT

The studied Mn-Fe ore deposits always tend to occupy a particular stratigraphic horizon, representing the lower member of Um Bogma Formation which belongs to the Lower Carboniferous. Mn-Fe ore deposits at Um Bogma area do not show the uniform characteristics of beds either in thickness or in lateral continuity. In some occurrences, the ore bodies are present as sills, veins, fracture filling and also found on the normal fault plane. All of these field criteria reveal hydrothermal origin of Mn-Fe ore deposits at Um Bogma area. Mineralogically, kaolinite mineral is recorded in the studied Mn-Fe ore deposits in the four localities, also Hausmanite and manganite detected in some localities (Allouga and Um Bogma) for the first time indicating hydrothermal origin. The suggestion of hydrothermal origin is further supported by the enrichment of Ba, Zn, Pb, As, U, V, Cu, and Sr, and depletion in Na, Mg, K, Ca and Ni in the studied Mn-Fe ore deposits. The studied Mn-Fe ore deposits show low Σ REEs contents, enrichment in LREEs relative to HREEs and strong negative Ce anomalies. Also, all of these geochemical data confirm the hydrothermal origin. In many localities manganese-iron ore bodies have spots reflecting high radioactivity reaches up to 527 ppm of eU. The average of eU/eTh ratio for the studied samples of Mn-Fe ore deposits of the four localities ranges between 4.0 up to 5.6 provide hydrothermal origin or may be later hydrothermal enrichment of the manganese ore. Sayrite, thorite and uranothorite represents the radioactive minerals detected in the studied Mn-Fe ore. Pinakiolite, rinmanite, turquoise, aheylite and gold also detected as accessory minerals.

INTRODUCTION

Um Bogma area is located about 40 Km east of Abu Zeneima town, Southwestern Sinai on the eastern coast of the Gulf of Suez. The area is bounded between long. 33° 20' & 33° 25' E and lat. 28° 57' & 29° 05' N (Fig. 1). The studied area is topographically moderately mountainous such as Gabal Allouga, G. Um Bogma, and G. Um Hamd and dissected by numerous wadis such as Wadi Lehian, W. Nasib, W. El-Sahu and W. Um Hamd. These wadies are structurally controlled by the NW, N-S and EW fault lines (Fig. 1).

The study area is characterized by its polymetallic mineralization since the Ancient Egyptians, especially copper and turquois. Recently this area became famous for Mn-Fe ores and some industrial minerals such as kaolin and glass sand.

Manganese-iron ore deposits are widely occur at some localities in Um Bogma area. These occurrences are considered the most important area in Egypt for manganese production. The geology and mineralogy of the manganese deposits of west central Sinai have been previously studied by various in-

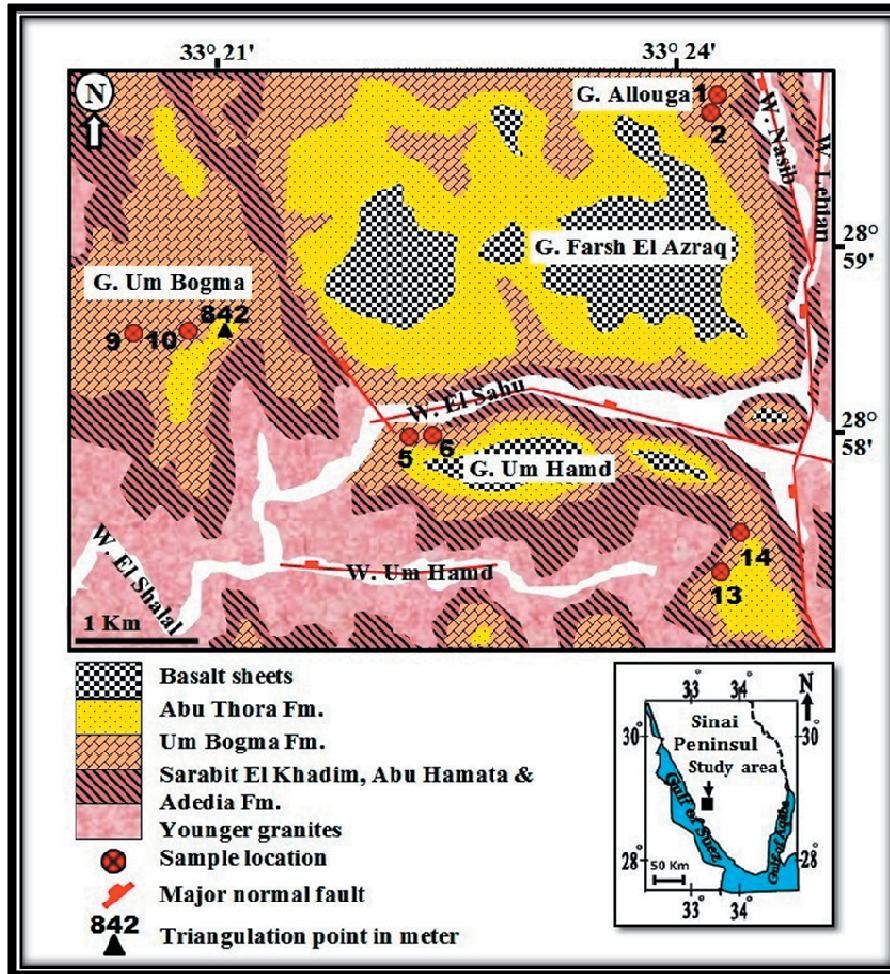


Fig. 1: Geological map of Um Bogma area

investigators (Mart and Sass 1972; Magaritz and Brenner 1979; Saleeb-Roufai et al., 1987; Khalil 1988). The origin problem of the studied manganese deposits hosted by carbonates still remains in dispute.

Two main theories were defined, the first proposed an epigenetic origin related to the activity of ascending mineralized hydrothermal solutions through the host rock, (Ball,

1916; Attia, 1956; Gindy 1961; Soliman, 1961; Nakhla and Shehata 1963; Weissbrod, 1969; Saad et al., 1991; Bishr and Gabr 2012; Shata and El Balakassy, 2012). It is based on the close spatial relationship between the Mn-Fe ore and its immediate neighborhood faults along which the ore deposits are found thicker and richer in manganese.

The second theory assumes a primary

sedimentary-type of manganese ore, in which the accumulation of the Mn-Fe deposits in a shallow marine basin separated from the open sea by a reef barrier and the main metal source was the outcrops of the Precambrian basement rocks (El Shazly et al., 1963; Mart and Sass; 1972; Magaritz and Brwennner, 1979; Kora 1984; ElAgamy et al., 2000). They gave the following considerations to support their theory: 1) The ore deposits always occupy the same stratigraphic horizon. 2) These deposits are older than the predominant faulting and folding in the district. In some cases, the deposits are cut and displaced by faults. 3) The association of pyrolusite, manganite and psilomelane with goethite and hematite characterizes the sedimentary deposits.

Recently, El-Sharkawi et al. (1990) demonstrated the role of weathering in the accumulation of the manganese deposits during the mature stage of Carboniferous karstification. Highly oxidized ore minerals, abrupt contacts between ore and carbonate country rocks and the strong enrichment of quartz sand grains in the ores is evidence of a karst-related mineralization. Shata and El Balakassy (2012) related uranium enrichment and other mobile trace elements within the present karst profiles, including the Mn-Fe ore to the supergene processes. The distribution of trace elements in manganese deposits is a useful criterion in any attempt to interpret the mode of their formation (Strakhov et al. 1967; Roy 1981).

The present study discussed the origin of ferromanganese ore at Um Bogma area based on detailed field investigation, radioactivity, chemical and mineralogical studies.

MATERIALS AND METHODS

Samples of unweathered uraniferous manganese ore deposits were carefully selected from spots distributed regularly over wide parts at four localities of the Um Bogma area Mn-Fe deposits. These localities are: Al-louga, El Sahu, Um Bogma and Um Hamd (Fig. 1). Field radiometric measurements

were performed using a handheld gamma-ray spectrometer (Model Rs-230 BGO Super-Spec, Radiation Detection Systems AB, Backehagen, Sweden) for the determination of eU (ppm), eTh (ppm) and K%. The frequency for acquiring radiometric measurements was set every 30 s. Mention the spacing of measurements in field (is constant spacing on grid pattern or random)

The mineralogical investigations were carried out in the Central Laboratories of the Nuclear Materials Authority (NMA), Cairo, Egypt. Three to five kgs of selected samples were crushed and sieved to collect the fraction 0.074 mm-0.5 mm, 35-200 Mesh). The sieved fraction was submitted to two separation steps: (a) densitometry separation using bromoform (Sp.G.: 2.85-2.89), (Quinif et al. 2006) and (b) magnetic separation using a Frantz Isodynamic Magnetic Separator (S.G. Frantz Co., Inc, Tully town, PA, USA). For magnetic separation, the side slope was set at 5° and the forward slope at 20° under and amperage of 0.5 A (Flinter 1959). Separated fractions were picked using binocular microscope (Meiji, Japan), and investigated with Environmental Scanning Electron Microscope ESEM (XL30-ESEM, Philips, FEI, Thermo Fisher Scientific, Hillsboro, OR, USA) associated with attached energy dispersive X-ray spectrometer (EDX) unit, was operated at 25–30 kV accelerating voltage, 1–2 mm beam diameter and 60–120 s counting time.

Also the mineralogical investigations were carried out in the C2MA at IMT–Mines Ales, France. In which the X-ray diffraction (XRD) data were collected using a BRUKER Advance D8 diffractometer in a θ - θ configuration employing the CuK α radiation ($\lambda=1.54\text{\AA}$) with a fixed divergence slit size 0.6° and a rotating sample stage. The samples were scanned between 4° and 70° with the Lynx-eye-1 detector, USA.

Polished sections were specifically analyzed using a Quanta FEG200, FEI-France, Thermo Fisher Scientific, Merignac, France)

coupled with an Oxford Inca 350 EDX microanalyzer (Oxford Instruments France, Saclay, France) at IMT–Mines Ales, France.

The determination of gold content required specific procedure; fire assay analysis were carried out at the Central Laboratory Sector of the Egyptian Mineral Resources Authority (EMRA). Fifty grams of samples (crushed and sieved to 200 Mesh) were fired in the presence of alkali fusion agents. More specifically the grinded sample was added to a mixture of litharge, borax, sodium carbonate, flour, silica and silver in a ceramic crucible. The mixture was melt at 1000 °C for 90 min; this step was followed by the cupellation of lead/gold/silver alloy at 900 °C for 60 min. The resulting alloy (Ag/Au) was then dissolved with concentrated nitric acid and aqua regain under heating to dissolve gold; the solution was further analyzed by atomic absorption spectrometry (using a Savant AA spectrometer, GBC Scientific Instruments, Braeside, Australia).

The chemical concentrations of the major oxides were determined using Shapiro and Branock (1962) methods. Inductively coupled plasma optical emission spectrometry (720 ICP-OES Agilent Technologies, Santa Clara, CA, USA) was used for measuring uranium and trace elements. These analyses were carried out at the Central Laboratory Sector of the Egyptian Mineral Resources Authority (EMRA). Mineral samples (crushed and sieved to 200 Mesh) were digested in teflon crucibles using 0.5 gm of grinded sample with 3 mL of perchloric acid, 5 mL of nitric acid and 15 mL of hydrofluoric acid: the mixture was covered with a glass lens and heated for 3 hours till complete digestion; in a second step the glass lens was removed to evaporate silica tetrafluoride till complete evaporation. Five mL of concentrated HCl were added to dissolve the solid residue; after drying under heating the solid was completely dissolved with 50 mL HCl aqueous solution (1:1 w/w); the volume was adjusted to 100 mL with distilled water and the concentration of metal ions analyzed by ICP-AES (720 ICP-OES, Agilent

Technologies, Santa Clara, CA, USA).

GEOLOGIC SETTING

Um Bogma area is covered mainly by basement rocks, comprise granites, gneisses and schists. The Paleozoic succession unconformably overlies the basement with a separating thin layer of basal conglomerate. The Paleozoic succession in some places is capped by Mesozoic basaltic sheets.

The succession is classified into the following formations starting from the oldest: Sarabit El Khadim, Abu Hamata and Adedia formations representing the lower clastic or sandstone series. This is followed unconformably overlain by Um Bogma Formation representing the middle carbonate series which is unconformably overlain by Abu Thora Formation representing the upper clastic or sandstone series. The importance of Um Bogma Formation attributed to hosting most of polymetallic mineralization occur within Paleozoic rocks, it is classified into three members: Lower member comprising ferruginous siltstones, claystone and sandy dolostone; middle member comprising marly dolostone, and upper member comprising sandy dolostone, claystone and ferruginous siltstones. The uranium mineralization is mainly associated with the middle member of Um Bogma Formation (El Aassy et al., 1986; El Agami, 1996 and Ashami, 2003).

The studied Mn-Fe ore deposits always tend to occupy a particular stratigraphic horizon, representing the lower member of Um Bogma Formation which belongs to the Lower Carboniferous. The individual ore bodies vary in length and thickness with irregular shape, tending to be lenticular. Sometimes Mn-Fe ore in some parts hosting ferruginous sandstones of the Adedia Formation as enclaves (Fig. 2). They don't show the uniform characteristics of bedding either in thickness or in lateral continuity. In some occurrences, the ore bodies are present as sills and veins cutting Abu Hamata and Adedia formations (Figs.

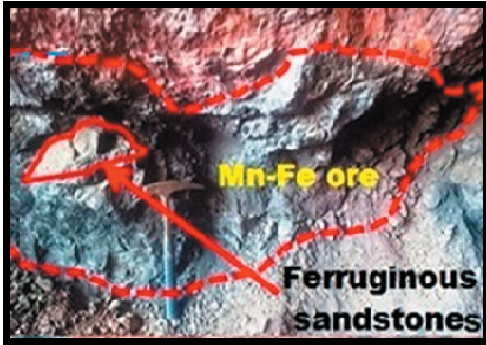


Fig. 2: Lens of Mn-Fe ore body hosting ferruginous sandstones of Adedia Fm., Allouga locality



Fig. 4: Vein of Mn-Fe ore invaded in Adedia Fm., Um Hamd locality

3&4), and also as irregular veins and sills invaded in El Hashash Formation (Figs. 5&6). Mn-Fe ore occur on the normal fault planes trending NW-SE (Fig. 7) cutting through Abu Hamata and Um Bogma formations. Sometimes manganese forms a dendritic shape on the fracture surface of the sandstones of Abu Hamata and Adedia formations (Figs. 8&9) and as irregular fracture filling in Adedia Formation (Fig. 10).

Mn-Fe ore usually present in a massive crystalline form (Fig. 11), also several forms characterize the constituents of the ore deposits such as granular, nodular, botryoidally (Fig. 12), fibrous (Fig. 13), radiating and needle-like

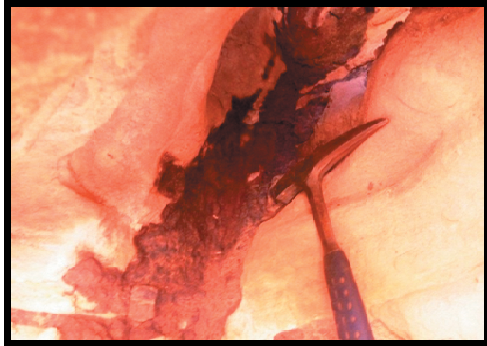


Fig. 5 : Irregular veins invaded in El Hashash Fm., Um Hamd locality



Fig. 3: Sill of Mn-Fe ore invaded in Abu Hamata Fm., Um Hamd locality



Fig. 6: Irregular sills invaded in El Hashash Fm., Um Hamd locality

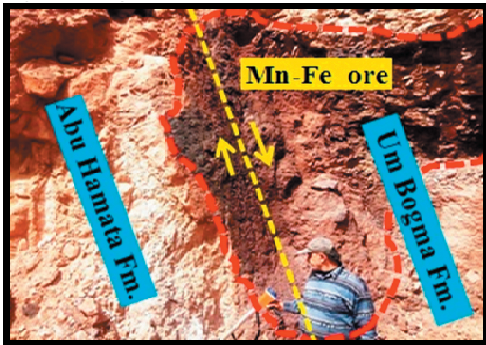


Fig. 7: Mn-Fe ore on the normal fault plane, Um Hamd locality



Fig. 10: Irregular fracture filling of Mn-Fe in Adedia Fm., El Sahu locality



Fig. 8: Dendritic Mn-Fe on the fracture surface of Abu Hamata Fm., El Sahu locality



Fig. 11: Massive crystalline Mn-Fe ore



Fig. 9: Dendritic Mn-Fe on the fracture surface of Adedia Fm., El Sahu locality



Fig. 12: Botryoidally forms of Mn-Fe ore



Fig. 13: Fibrous forms of Mn-Fe ore



Fig. 14: Dark green copper mineralization filling the vogues of the manganese ore body, Allouga locality

crystals. The ore body varies in composition from high grade manganese ore to low grade ore according to the Mn-contents relative to the Fe-contents. Generally, manganese ore represents a mixture of the Mn and Fe in variable concentrations.

Many types of mineralization were detected as spots in association with Mn-Fe ore body. Dark green highly radioactive copper mineralization were recorded filling the vogues and fractures as well as staining on wall of the manganese ore body (Fig. 14) reflecting hydrothermal activity and its late timing with respect to the forming of the ore body. Also, some radioactive mineralization was detected filling fractures and vogues with yellow and green colour. Turquoise is present as very fine rounded whitish blue particles disseminated within the Mn-Fe ore body as well as veinlets (Fig. 15) at Allouga locality. High radioactive kaolin lens recorded in association with lens of manganese ore body (Fig. 16) with visible uranium mineralization (Fig. 17) at El Sahu locality.



Fig. 15: Veinlets of turquoise within Mn-Fe ore body, Allouga locality

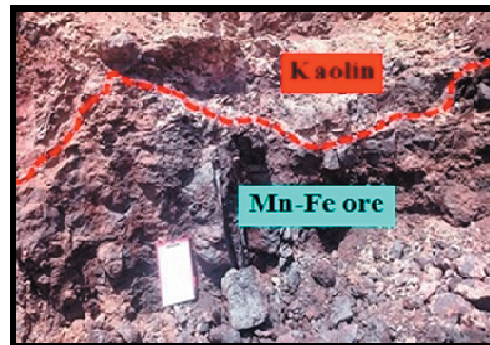


Fig. 16: Kaolin lens association with lens of manganese ore body, El Sahu locality

Faults are the main structural elements that left their prints on the rocks of the study area. They can be grouped into; NNW-SSE of normal faults (Red Sea rifting trend) along which the Permo-Triassic basaltic dykes were erupted and NW-SE trending faults (Gulf of Suez



Fig. 17: Visible uranium mineralization on Kaolin lens, El Sahu locality

rifting trend) along which the main wadies of Um Bogma area were incised including Wadi Nasib (Fig. 1). However the studied area comprises a mosaic of faulted blocks (Fig.18).

Alshami (2018) recorded that the NW-trending faults controlled the high U-concentration at Wadis Naseib, Taleet Seleim, Moreid and Abu Hamata, whereas the NE-trending faults controlled the U-concentrations at Wadi Baba. The E-W trending faults controlled the U-concentration at Wadi El Sahu. The Allouga is located at the down thrown block of the Nasib normal fault, and its high U-anoma-

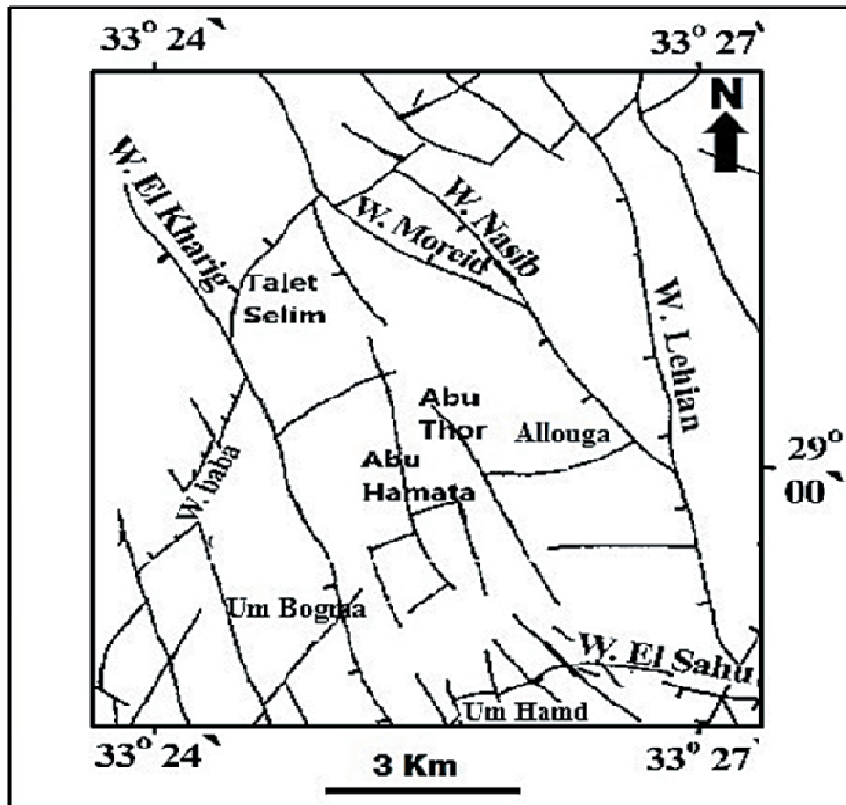


Fig. 18: Major faults of Um Bogma area (Modified after Alshami ,2018)

lies are controlled by its 2nd order fault system. The Southwestern Sinai district was affected by two volcanic episodes. The early one belongs to the Permo-Triassic age and was manifested by the basaltic sheet and/or sill at the top of the Post-Miocene age and resulted in abundant dolerite and basaltic dikes (El Shazly and Saleeb, 1969).

RADIOACTIVITY

The average eU-contents in Mn-Fe ore body in different localities at Um Bogma area not exceed 15 ppm with average eTh-contents reaches 7 ppm. In many localities Mn-Fe ore body has spots reflecting high radioactivity. These spots vary in dimension from 0.2 x 0.3 m to 1 x 1.5 m with radioactive intensity reaches 527 ppm (eU) in some localities (Table 1).

The eU/eTh ratio is a very important geochemical index for U migration in or out, it is approximately constant in the same rock type or geologic unit in relatively closed environ-

ment. The Clark value for eU/eTh in the sedimentary rocks is equal 1(Clark, et al. 1966). The average of eU/eTh ratio of the studied anomalous Mn-Fe ore varies between 4.0 to 5.6 times Clark value, these reveals that the studied anomalous manganese ore has migration in (enrichment) of uranium. The presences of manganese and iron minerals are playing an important factor in capture of uranium.

D-factor is equal to the ratio of the chemically measured uranium (Uc) to radiometrically measured uranium (eU), if this factor was more or less than unity; it indicates disequilibrium state which, could be due to an addition or removal of U (Hansink, 1976). Chemical measurements of uranium contents of the anomalous facies are slightly lower than those of field radiometric measurements (Table 1). This indicates that all the studied anomalous ore are in slightly negative disequilibrium state due to a removal of uranium. This means that some of uranium in these rocks has been removed leaving the daughter products behind, hence the level of radioactivity is higher

Table 1: Field radiometric and chemical measurements of radioactive Mn-Fe ore,Um Bogma area.

Sample No.	Locality	Rock type	Age	Fm.	Member	eU (ppm)	eTh (ppm)	Uc (ppm)	Uc/eU	eU/eTh				
1	Allouga	Radioactive Mn-Fe ore	Lower Carboniferous	Um Bogma	Lower	527	87	485	0.9	6.1				
2						436	81	395	0.9	5.4				
3						468	92			5.1				
4						458	77			5.9				
Average									472.3	84.3	440	0.9	5.6	
5	El Sahu									415	101	389	0.9	4.1
6						366	73	350	0.9	5.0				
7						387	71			5.5				
8						297	65			4.6				
Average									366.3	77.5	369.5	0.9	4.8	
9	Um Bogma									377	55	251	0.7	6.9
10						256	69	229	0.9	3.7				
11		280	53			5.3								
12		359	74			4.9								
Average					318	62.8	240	0.8	4.0					
13	Um Hamd					230	75	194	0.8	3.1				
14		190	48	167	0.9	4.0								
15		319	67			4.8								
16		249	59			4.2								
Average					247	62.3	180.5	0.8	4.0					

than would be expected for the amount of uranium present.

The eU/eTh ratio may be used to discriminate hydrothermal deposits from sedimentary (Bonatti, 1975) in which more than unity means addition of uranium indicating hydrothermal origin. The average of eU/eTh ratio for the studied samples of Mn-Fe ore deposits of the four localities ranges between 4.0 up to 5.6 provide hydrothermal origin or may be later hydrothermal enrichment of the manganese-iron ore.

Generally, the probable origin of the radioactive anomalies recorded in the study Mn-Fe ore bodies could be attributed to the epigenetic concept, in which, the secondary ascending hydrothermal solutions carry out the radioactive elements to deposit mainly along fractures and fault plains. In addition to leaching concept; in which, the uranium has been leached from other surrounding rocks, transported by means of circulating water and finally captured by manganese and iron minerals. The lithology, structure and topography played an important role in localization of uranium and associated elements (Alshami, 2017).

MINERALOGY

Manganese Minerals

Hausmanite(Mn_3O_4)

It is a primary mineral usually exists in hydrothermal veins. Hausmanite detected in Allouga and Um Bogma localities. It was detected by using of X-ray diffraction technique (XRD) (Fig. 19).

Manganite [$MnO(OH)$]

It is formed in low-temperature hydrothermal or hot-springs manganese deposits. It detected by using of XRD technique (Fig. 19). The presence of hausmannite and manganite minerals is indication of hydrothermal activ-

ity (Brugger et al., 2001).

Cryptomelane($K_2Mn_8O_{16}$)

It is widespread in oxidized manganese deposits as open-space fillings or replacing primary manganese-bearing minerals. Cryptomelane is detected by using of XRD technique (Fig. 19).

Pyrolusite(MnO_2)

It is formed under highly oxidizing conditions in manganese-bearing hydrothermal deposits, commonly an alteration product of manganite. Pyrolusite is detected by using of XRD technique (Figs. 19&24). Shata and El Balakassy (2012) detected hydrogen-autunite and carnotite uranium minerals disseminated in the interspaces of pyrolusite radial and acicular grains.

Ronneburgite ($K_2MnV_4O_{12}$)

It is low-temperature alteration product formed under oxidizing conditions. Ronneburgite is present as subhedral reddish-brown crystals detected by using of XRD technique (Fig. 20).

Iron Minerals

Hematite (Fe_2O_3)

Generally, hematite occurs in volcanic rocks, and in high-temperature hydrothermal veins. Hematite is detected by using of XRD technique (Fig. 19).

Goethite [$FeO(OH)$]

It is a common weathering product derived from numerous iron-bearing minerals in oxygenated environments. Goethite is detected by using of XRD technique (Fig. 19).

Minnesotaite [$(Fe, Mg)_{27}Si_{36}O_{86}(OH)_{26}$]

It is greenish-gray unihedral crystals detected by using of XRD technique (Fig. 19).

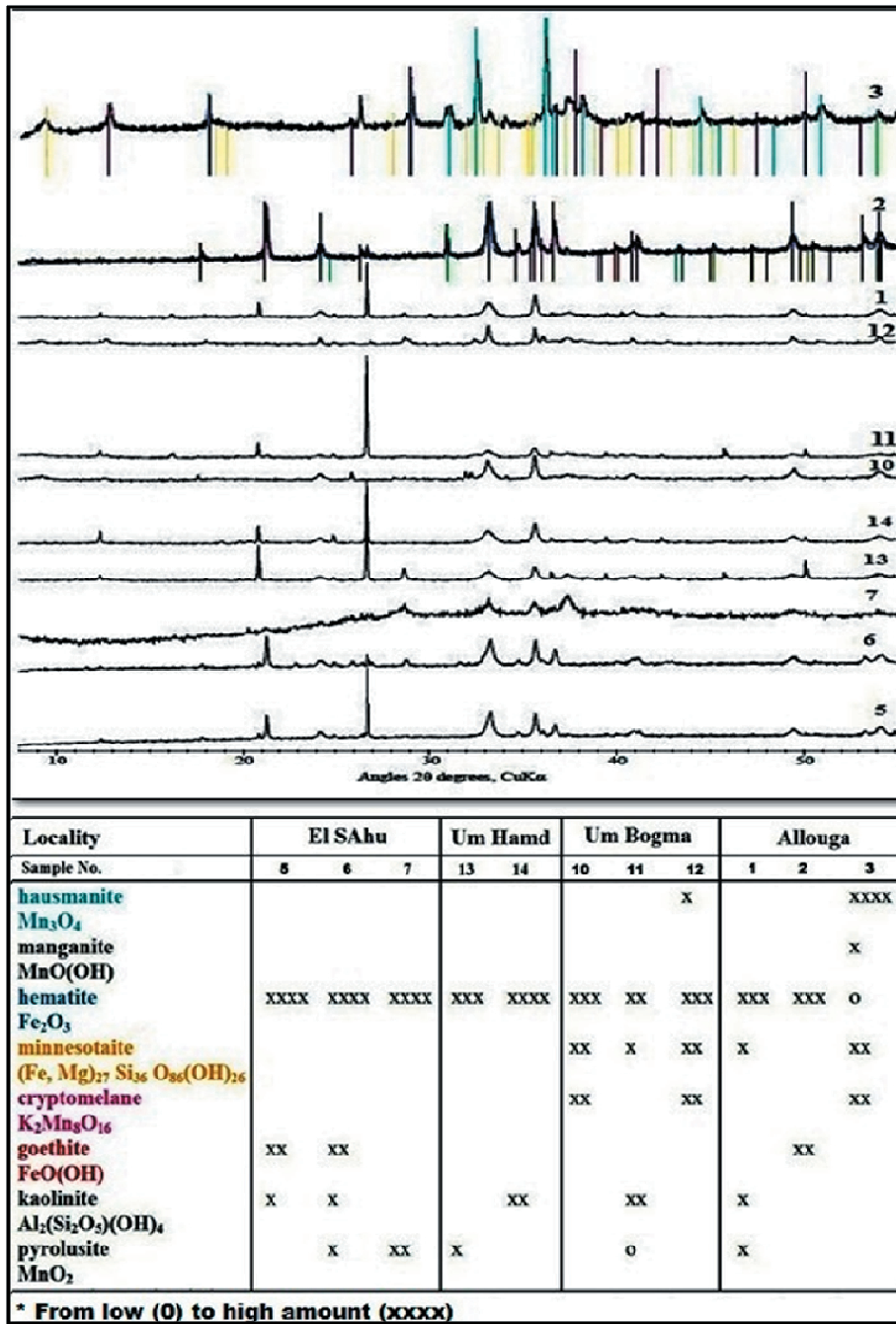


Fig. 19: X-ray diffraction patterns of some minerals of Mn-Fe ore, Um Bogma area

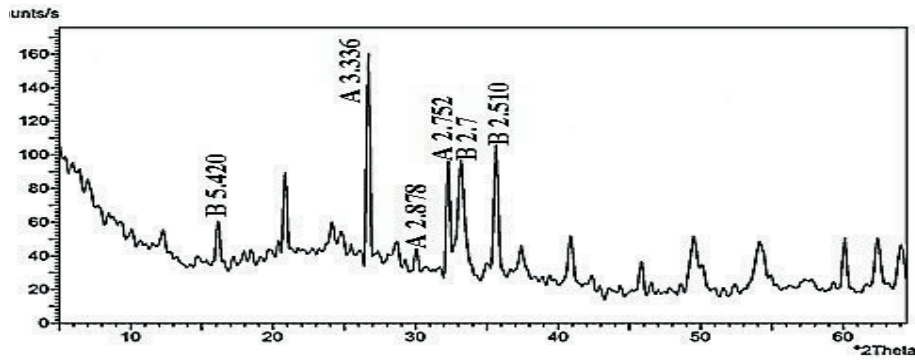


Fig. 20: X-ray diffraction pattern of ronneburgite (A) and pinakiolite (B) minerals in Mn-Fe ore, Um Bogma area

Tetrataenite (FeNi)

It is formed by hydrothermal alteration of ferromagnesian minerals. Tetrataenite is detected by using of XRD technique (Fig. 21).

Trevorite ($\text{NiFe}^{3+}_2\text{O}_4$)

It is a hydrothermal mineral occurs as black subhedral crystals and detected by using of XRD technique (Fig. 9).

Radioactive Minerals

Sayrite [$\text{Pb}_2(\text{UO}_2)_5\text{O}_6(\text{OH})_2 \cdot 4\text{H}_2\text{O}$]

It is an alteration product of uraninite in the oxidized zone of a uranium ore body. Say-

rite is detected by using of XRD technique (Fig. 21).

Thorite and uranothorite [$(\text{Th;U})\text{SiO}_4$]

They are detected by using of XRD and Environmental Scanning Electron Microscope (ESEM) techniques respectively (Fig. 22 & 23).

Accessory Minerals

Pinakiolite [$(\text{Mg}, \text{Mn}^{2+})_2(\text{Mn}^{3+}, \text{Sb}^{5+})\text{BO}_3$]

It is a rare mineral in a metamorphosed Fe-Mn ore body. Pinakiolite is detected by using of XRD technique (Fig. 20).

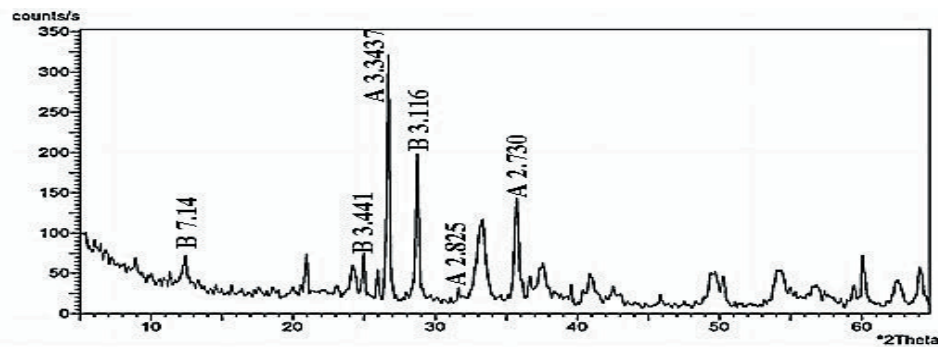


Fig. 21: X-ray diffraction pattern of tetrataenite (A) and sayrite (B) minerals in Mn-Fe ore, Um Bogma area

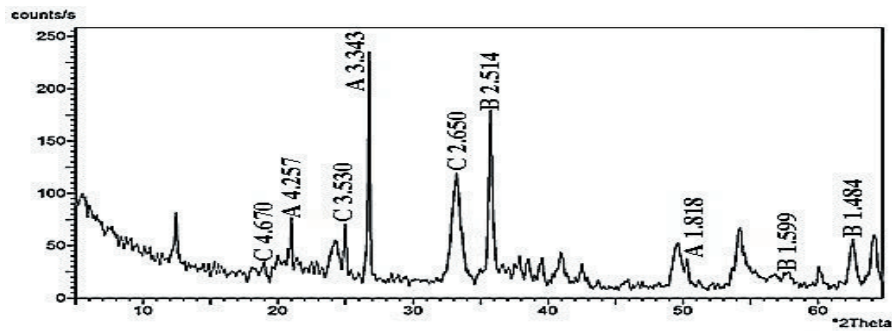


Fig. 22: X-ray diffraction pattern of quartz (A), tevorite (B) and andthorite (C) minerals in Mn-Fe ore, Um Bogma area

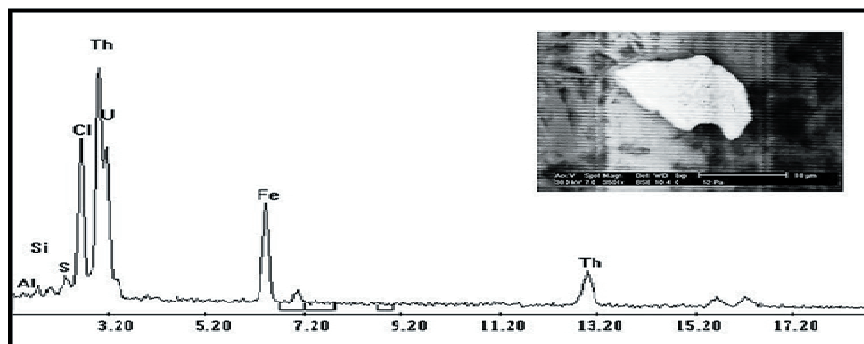


Fig. 23: EDX spectrum and BSE image showing uranothorite mineral in Mn-Fe ore, Um Bogma area

Kaolinite $[\text{Al}_2\text{Si}_2\text{O}_5(\text{OH})_4]$

It exists in some Mn-Fe studied samples of all localities. Kaolinite detected by using of XRD technique (Fig. 19). The detection of kaolinite prevailing in the manganese deposits is a good indicator for hydrothermal genesis (Saad et al., 1991).

Rinmanite $(\text{Zn}_2\text{Sb}_2\text{Mg}_2\text{Fe}^{3+}_4\text{O}_{14}(\text{OH})_2)$

It is a secondary mineral in marine saline evaporite deposits detected by using of XRD technique (Fig. 24).

Turquoise $[\text{CuAl}_6(\text{PO}_4)_4(\text{OH})_8 \cdot 4\text{H}_2\text{O}]$

It is present as blue-to-green subhedral crystals and detected by using of XRD tech-

nique (Fig. 25). The blue is attributed to idiochromatic copper while the green may be the result of either iron impurities (replacing aluminium) or dehydration.

Aheylite $[(\text{Fe}^{2+}, \text{Zn})\text{Al}_6(\text{PO}_4)_4(\text{OH})_8 \cdot 4\text{H}_2\text{O}]$

It is a late stage hydrothermal mineral detected by using of XRD technique (Fig. 25).

Gold (Au)

Four samples (one from each locality) of the Mn-Fe ore of the lower member of Um Bogma Formation were analyzed for measuring their gold contents by using of fire assay analysis technique. Gold is detected only in the Allouga locality sample; the gold contents

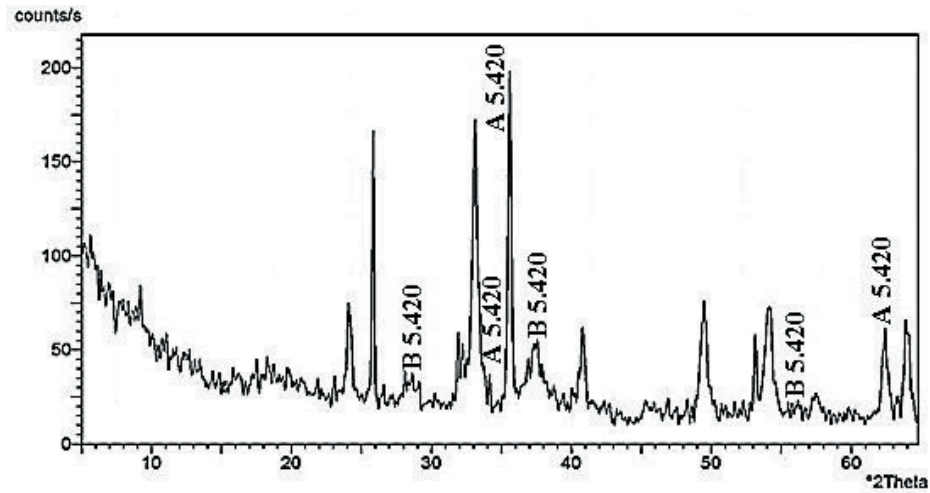


Fig. 24: X-ray diffraction pattern of rinmanite (A) and pyrolusite (B) minerals in Mn-Fe ore, Um Bogma area

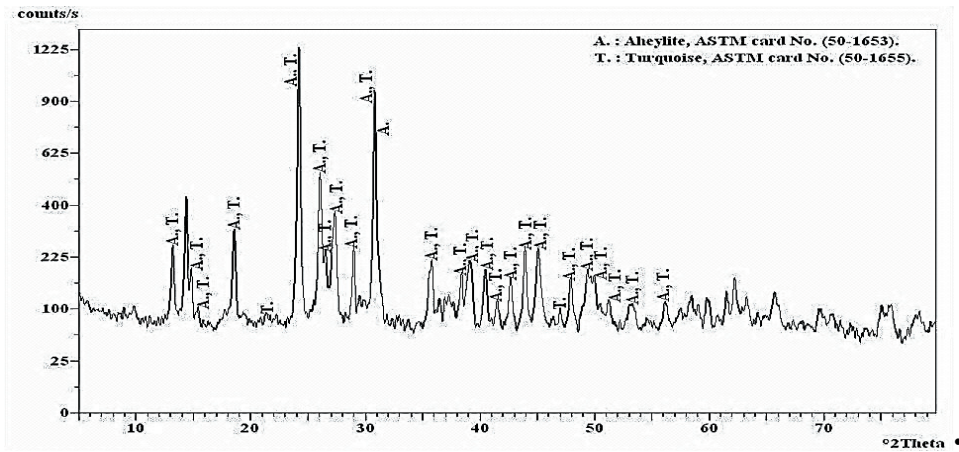


Fig. 25: X-ray diffraction pattern of turquoise and aheylite in Mn-Fe ore, Um Bogma area

reach 0.32 ppm. The identified gold may be from the hydrothermal deposits.

Polished sections were done for the sample which contains gold (Allouga locality sample) to study the gold by the scanning electron microscope. Gold is found as very fine grain enclosed in manganese ore mineral (pyro-

lusite) (Fig. 26) at Allouga locality. Gold is detected by using of ESEM technique (Fig. 27). Sallam et al. (2014) recorded minerals bearing Ag and Au namely uytenbogaardite and furutobeite in the lower member of Um Bogma Formation at El Sheikh Soliman area. Alshami (2019) detected gold in Um Bogma Formation at Allouga locality.



Fig. 26: Reflected light photomicrograph showing very fine grain of gold enclosed in manganese (pyrolusite) , XRL

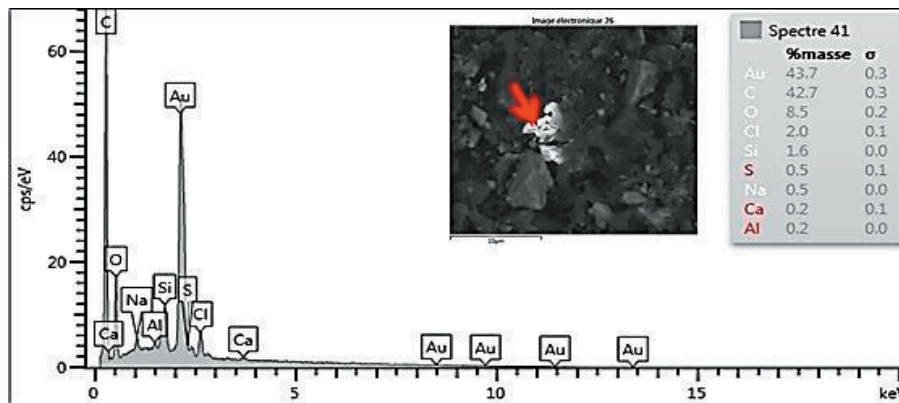


Fig. 27: EDX spectrum and BSE image showing gold in Mn-Fe ore, Um Bogma area

GEOCHEMISTRY

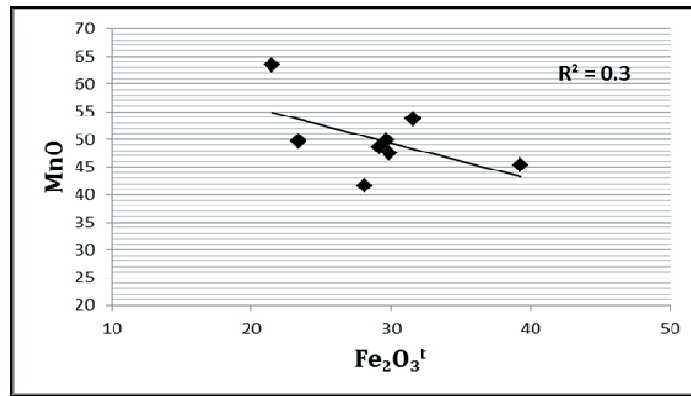
The chemical composition of the studied manganese deposits of the Um Bogma area is given in Tables 2, 3&4.

According to the major elements contents of the studied Mn-Fe ore deposits (Table 2), a reverse relation between the manganese and iron oxides contents exists in the analyzed

samples (Fig. 28). This reverse relation suggests that a fractionation between these two elements took place during their deposition. This process often takes place in submarine hydrothermal systems such as those well-known from the Santorini, the Red Sea and the Galapagos hydrothermal areas (Smith and Cronan 1975; Bignell et al., 1976; Varnavas 1979; Varnavas and Cronan 1981).

Table 2: Major oxides measurements (in %) of the studied Mn-Fe ore, Um Bogma area

Locality	Allouga		El Sahu		Um Bogma		Um Hamd	
Formation			Lower Um Bogma					
Rock type			Mn-Fe ore					
Sample No.	1	2	5	6	9	10	13	14
SiO ₂	5.8	8.9	11.5	12.8	9.7	7.3	13.5	11.3
Al ₂ O ₃	3.9	4.8	4.4	3.2	2.6	1.5	7.6	5.5
TiO ₂	0.03	0.15	0.07	0.09	0.15	0.92	0.62	0.89
Fe ₂ O ₃ ^t	31.6	29.7	39.3	29.9	23.4	21.5	28.1	29.2
MnO	53.7	49.8	45.4	47.5	59.7	63.4	41.7	48.6
CaO	0.9	0.7	0.6	2.4	0.7	0.8	0.4	1.2
Na ₂ O	0.7	0.9	0.4	0.6	0.9	0.2	0.7	0.8
K ₂ O	0.4	0.3	0.2	0.3	0.4	0.1	0.6	0.5
MgO	0.8	0.5	0.1	0.9	0.3	0.4	0.3	0.5
P ₂ O ₅	0.3	0.2	0.7	0.5	0.2	0.3	0.9	0.6
L.O.I.	1.7	2.4	1.4	1.7	1.0	2.9	4.3	1.5
Total	99.83	98.35	98.07	99.89	99.05	99.32	99.72	99.97

Fig. 28: MnO versus Fe₂O₃^t of Mn-Fe ore, Um Bogma area

The trace elements measurement (Table 3) of the studied Mn-Fe ore deposits show enrichment in Ba, Zn, Pb, As, U, V, Cu, and Sr. Nicholson (1992) recorded that hydrothermal manganese deposits are characterized by enrichment in Cu, Zn, Pb, V, As, Sr, Sb, Li, Mo, Cd and Ba, while that of sedimentary marine deposits reflect enrichment in Ca, Mg, Na, K, Sr, Co, Cu and Ni.

The presence of Pb may be attributed to the adsorption character of manganite, which is considered as a better adsorbent for Pb than for any other ion (Grassely and Hetengi 1971). The dominance of Zn is due to the presence

of rinmanite and aheylite or may be represented as a substantial element in the lattice of hausmannite (McSween 1976).

Many authors used the major and trace elements to differentiate between hydrothermal and sedimentary marine origin of the manganese ore deposits. According to the (Cu+Ni+Co)10-Fe-Mn ternary diagram of Bonatti et al. (1972) the studied samples of the manganese ore deposits fall in a field of the hydrothermal origin (Fig. 29). Also, by plotting the samples on the Zn versus Pb and As+Cu+Mo+Pb+V+Zn (Wt%) versus Co+Ni (Wt%) (Figs. 30&31) of Nicholson

Table 3: Trace elements measurements (in ppm) of the studied Mn-Fe ore, Um Bogma area.

Locality	Allouga			El Sahu	Um Bogma		Um Hamd	
Formation				Lower Um Bogma				
Rock type				Mn-Fe ore				
Sample No.	1	2	5	6	9	10	13	14
As	480	463	320	280	375	450	323	447
Co	129	78	149	115	87	169	151	113
Cu	315	210	275	330	117	198	220	125
Mo	8	10	6	7	9	8	5	7
Ni	6	-	-	91	4	-	-	8
Pb	560	730	280	517	358	616	411	153
V	340	318	321	210	274	344	217	225
Zn	945	1340	428	781	483	415	690	395
Ba	968	1050	790	854	1340	814	655	820
Sr	240	230	355	290	320	273	340	154
Cr	41	32	19	48	27	15	39	25
Nb	83	54	77	49	76	61	42	51
Ta	33	40	21	18	35	28	19	36
U	485	395	389	350	251	229	194	167

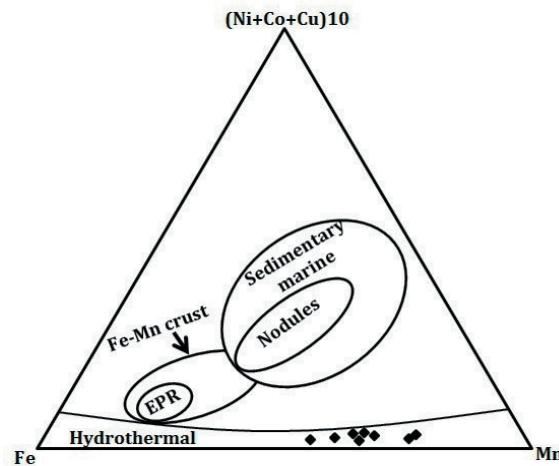


Fig. 29: Ternary diagram showing (Co+Ni+Cu)10-Fe-Mn of (Bonatti et al. 1972) for Mn-Fe ore, Um Bogma area

(1992) and Co/Zn (ppm) versus Co+Ni+Cu (ppm) diagram of Toth (1980) (Fig. 32) the studied manganese-iron ore fall in the field of hydrothermal origin.

The hydrothermal origin hypothesis is further supported by the relatively enrichment of Ba (reach up to 1340 ppm) in the studied Mn-Fe ore deposits. Ba is usually concentrated in hydrothermal micro-nodules from the deeper zone of Mn-Fe ore deposits

(Bonatti et al., 1972).

The concentrations and distribution of rare earth elements (REEs) in the studied manganese-iron ore deposits are shown in Table 4. \sum REEs contents range between 133.5 up to 377.3 ppm, these values are small compared with that of hydrogenetic crust, where the concentration more than 1400 ppm (Hein et al. 1997). While, low contents of REEs (\approx 100 ppm) are characteristic of hydrothermal man-

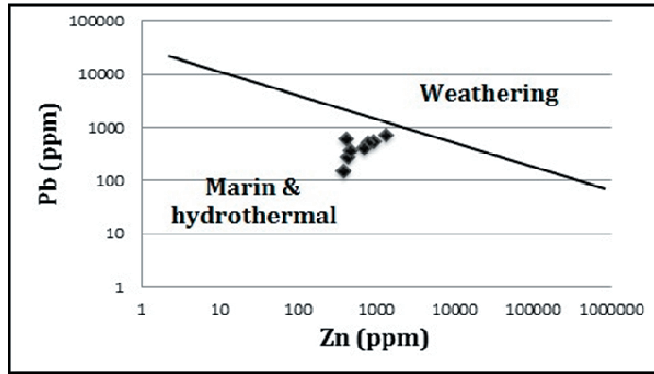


Fig. 30: Zn-Pb diagram of Nicholson (1992) for Mn-Fe ore, Um Bogma area

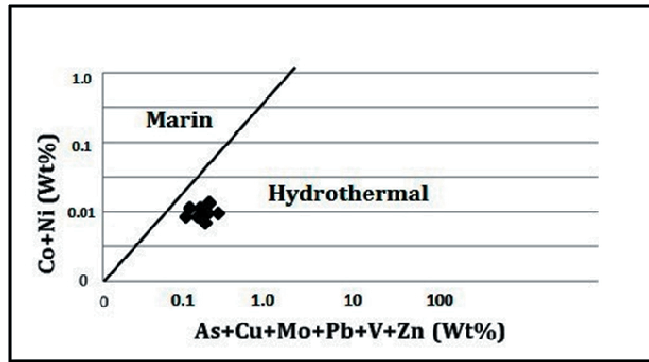


Fig. 31: As+Cu+Mo+Pb+V+Zn - Co+Ni diagram of Nicholson (1992) for Mn-Fe ore, Um Bogma area

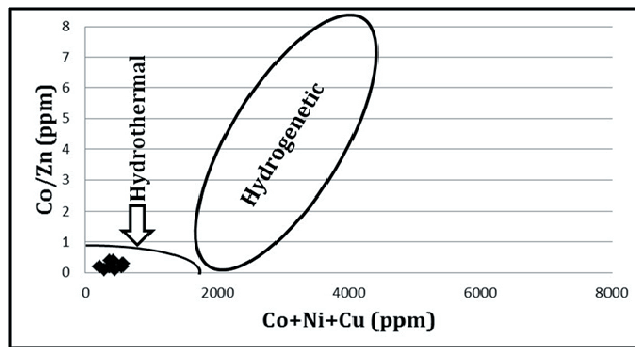


Fig. 32: Co/Zn - Co+Ni+Cu diagram of (Toth 1980) for Mn-Fe ore, Um Bogma area

ganese deposits (Usui et al. 1997).

REEs of the Um Bogma Mn-Fe ore deposits normalized to chondrite of Boynton, 1984 (Fig. 33) and Taylor and McLennan, 1985 (Fig. 34). According to chondrite patterns the studied Mn-Fe deposits show enrichment in LREEs relative to HREEs, in which the LREEs/HREEs ratios range between 3.5 to 7.7 (Table 4). The enrichment in LREEs in the studied Mn-Fe is considered also as indicator of hydrothermal origin (Mills and El-derfield 1995).

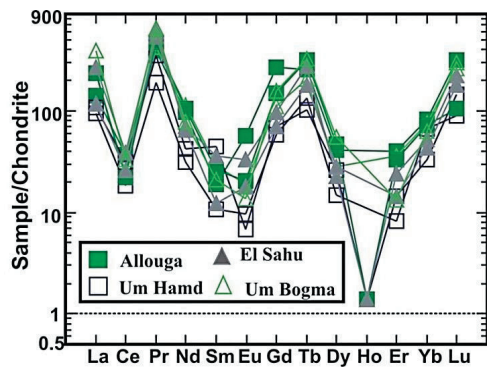


Fig. 33: Trace elements distribution pattern of the studied Mn-Fe ore, normalized to the Chondrite of Boynton, 1984

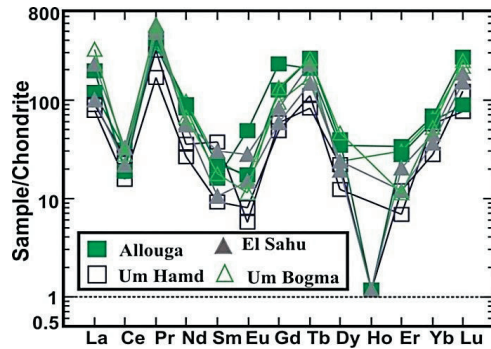


Fig. 34: Trace elements distribution pattern of the studied Mn-Fe ore, normalized to the Chondrite of Taylor and McLennan, 1985

Also REEs normalized with North American Composite Shale (NSCA) of Haskin and Haskin, 1966 (Fig. 35) and Gromet et al., 1984 (Fig. 36). In both diagrams the Mn-Fe ore deposits of Um Bogma area are showing strong negative Ce anomalies in their REE distribution diagrams. This indicates hydrothermal origin of mineralization (Graf 1977, Fryer 1977, Kato 1999, Jiangli 1999 a, b, Huawen et al., 2002, Canet et al., 2004, Fitzgerald and Gills 2006). Some samples show positive Eu anomaly, which also indicates the hydrothermal origin of the Mn-Fe ore deposits (Danielson et al., 1992, Jiang et al., 2004).

Table 4: Rare earth elements (REEs) measurements (in ppm) of the studied Mn-Fe ore, Um Bogma area

Locality Formation Rock type Sample No.	Allouga		El Sahu Lower Um Bogma Mn-Fe ore		Um Bogma		Um Hamd	
	1	2	5	6	9	10	13	14
La	44	73	36	84	120	75	29	33
Ce	30	18	21	31	27	19	15	25
Dy	13.2	15	7.3	9	17.5	9.1	4.7	8.3
Er	8.4	7	5.1	3	2.8	7.5	1.7	3
Eu	4.2	1.5	2.4	1.3	1	1.4	0.7	0.5
Gd	70	38	25	18	41	29	15	18
Ho	N.D	0.1	0.1	N.D	N.D	N.D	N.D	0.1
Lu	10.2	3.4	7.1	5.7	9.5	8.3	2.9	4.6
Nd	58	63	42	39	47	68	19	25
Pr	48	57	66	73	79	51	23	43
Sm	3.7	5.1	7	2.4	4.1	5.7	2.1	8.6
Tb	11.9	15.1	13.2	8.5	15.4	9.7	6.3	4.8
Tm	N.D	N.D	N.D	N.D	N.D	N.D	N.D	N.D
Yb	17	15	11	9	13	16	14	7
LREEs	257.9	255.6	199.4	248.7	319.1	249.1	103.9	153.1
HREEs	60.7	55.6	43.8	35.2	58.2	50.6	29.6	27.8
• REEs	318.6	311.2	243.2	283.9	377.3	299.7	133.5	180.9
L/H	4.3	4.6	4.6	7.7	5.5	4.9	3.5	5.5

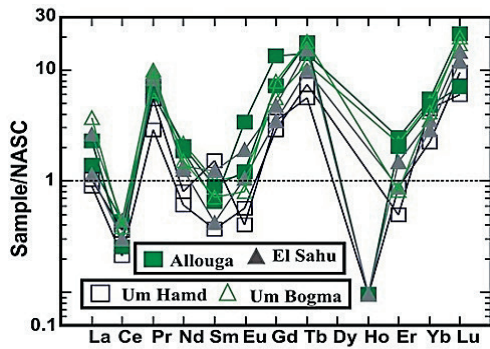


Fig. 35: Rare earth elements concentrations in the studied Mn-Fe ore as normalized to the North American Composite Shale (NASC), (Haskin and Haskin, 1966)

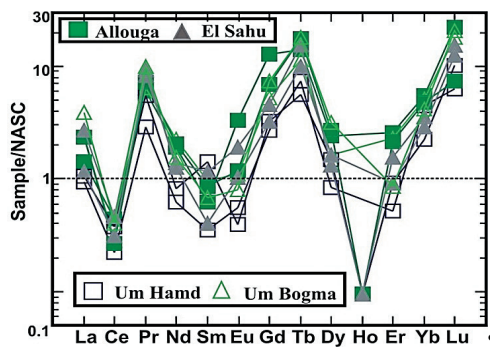


Fig. 36: Rare earth elements concentrations in the studied Mn-Fe ore as normalized to the North American Composite Shale (NASC), (Gromet, 1984)

DISCUSSION

The studied Mn-Fe ore deposits always tend to occupy a particular stratigraphic horizon, representing the lower member of Um Bogma Formation which belongs to the Lower Carboniferous age. Mn-Fe ore deposits at Um Bogma area do not show the uniform characteristics of bedding either in thickness or in lateral continuity. In some occurrences, the ore bodies are present as sills, veins, frac-

ture filling and also found on the normal fault planes.

Mineralogically, kaolinite mineral is recorded in the studied Mn-Fe ore deposits in the four localities, also Hausmanite and manganese detected in some localities (Allouga and Um Bogma) for the first time indicating hydrothermal origin.

The hydrothermal origin suggestion is further supported by the enrichment of Ba, Zn, Pb, As, U, V, Cu, and Sr, and depletion in Na, Mg, K, Ca and Ni in the studied Mn-Fe ore deposits. Σ REEs contents range between 133.5 up to 377.3 ppm, these values are relatively small and are characteristic of hydrothermal manganese deposits. The studied Mn-Fe deposits show enrichment in LREEs relative to HREEs, in which the LREEs/HREEs ratios range between 3.5 and 7.7. The enrichment in LREEs in the studied Mn-Fe is considered also as indicator of hydrothermal origin. The Mn-Fe ore deposits of Um Bogma area are showing strong negative Ce anomalies, this indicates hydrothermal origin of mineralization.

In many localities manganese-iron ore bodies have spots reflecting high radioactivity reaches 527 ppm of eU. The average of eU/eTh ratio for the studied samples of Mn-Fe ore deposits of the four localities ranges between 4.0 up to 5.6 provide hydrothermal origin or may be later hydrothermal enrichment of the manganese ore. Sayrite, thorite and uranothorite the radioactive minerals which detected in the studied Mn-Fe ore. Pinakio-lite, rinmanite, turquoise, aheylite and gold also detected as accessory minerals.

CONCLUSIONS

According to the field criteria, mineralogical and chemical data in this study the Mn-Fe ore deposits at Allouga, Um Bogma, El Sahu and Um Hamd localities have a hydrothermal origin.

Acknowledgements

The author acknowledges the support of Nuclear Materials Authority, Cairo, Egypt, for their kind field and laboratory facilities during the preparation of this work.

Thanks are extended to the support of the IMHOTEP project MetalValor (funded by the French Government through the Institut Français d'Égypte and by the Egyptian Academy of Scientific Research).

REFERENCES

- Alshami, A.S., 2003. Structural and lithologic control of uranium and copper mineralization in the Um Bogma environs, southwestern Sinai, Egypt. Ph.D. Thesis, Fac. of Sci., Mansoura Univ., Egypt, 205p.
- Alshami, A.S., 2018. U-minerals and REE distribution, paragenesis and provenance of Um Bogma Formations, southwestern Sinai, Egypt. Nuclear Sciences Scientific Journal, <http://www.ssnma.com>, 7, 31 – 55.
- Alshami, A.S., 2019. Infra-cambrian placer gold-uraniferous Paleozoic sediments, southwestern Sinai, Egypt. Nuclear Sciences Scientific Journal 8, 1-16. <http://www.ssnma.com>
- Attia, M.I., 1956. Manganese deposits of Egypt: Symposium de la manganese: 20th International Geological Congress, Africa, 2, 143-171.
- Ball, J., 1916. The Geography and Geology of West Central Sinai, Egypt. Survey Dept., Cairo, 219p.
- Bignell, R.D., Cronan, D.S., and Tooms, J.W., 1976. Metal dispersion in the Red Sea as an aid to marine geochemical exploration. Transactions Institution Mining Metallurgy, 85, 274-278.
- Bishr, A.H., and Gabr, M.M., 2012. Geological and mineralogical evidences for the origin of Mn-Fe and U mineralizations in Talet Seliem area, southwestern Sinai, Egypt. Sedimentology of Egypt, 20, 27-33.
- Bonatti, E.; Kraemer, T., and Rydell, H., 1972. Classification and genesis of submarine iron-manganese deposits. In: Horn, D., ed., Ferromanganese deposits on the ocean floor. D.C. Washington, Natl. Sci., Found., 49-166.
- Bonatti, E., 1975. Metallogenesis at Oceanic Spreading Centers, Ann. Rev. Earth and Planetary Sciences, 3, 401-431.
- Boynton, W.V., 1984. Cosmochemistry of the rare earth elements; meteorite studies. In: Rare earth element geochemistry (Henderson, P., Ed.), Elsevier Sci. Publ. Co., Amsterdam, 63-114.
- Brugger, J.; Armbruster, T.; Criddle, A.J.; Berlepsch, P.; Graeser, S., and Reeves, S., 2001. Description, crystal structure, and paragenesis of krettnichite, $PbMn_3+2(VO_4)_2(OH)_2$, the Mn³⁺ analogue of mounanaite. Eur. J. Mineral. 13, 145-158.
- Canet, C.; Alfonso, P.; Melgarejo, J.C., and Belyatsky, B.V., 2004. Geochemical evidences of sedimentary-exhalative origin of the shale-hosted PGE-Ag-Au-Zn-Cu occurrences of the Prades Mountains (Catalonia, Spain): trace element abundances and Sm-Nd isotopes. J. Geochem. Explor., 82, 17-33.
- Clark, S.P., Peterman, Z.E. and Heier, K.S., 1966. Abundance of uranium, thorium and potassium. In: Handbook of Physical Constant (S.P. Clarke, Jr., Ed.), Geol. Soc. Am. Mem. 97, Section, 24, 521-541.
- Danielson, A.; Möller, P., and Dulski, P., 1992. The europium anomalies in banded iron formation-sand the thermal history of the oceanic crust. Chem. Geol., 97, 89-100.
- El Aassy, I.E.; Botros, N.H.; Abdel Razik, A.; Alshamy, A.S.; Ibrahim, S.K.; Sherif, H.Y.; Attia, K.E., and Moufeï, A.A., 1986. Report on proving of some radioactive occurrences in west central Sinai. Int. Rept. N.M.A., Cairo, Egypt.
- El Agami, N.L., 1996. Geology and radioactivity studies on the Paleozoic rock units in Sinai Peninsula, Egypt. Ph.D. Thesis, Fac. Sc., Mansoura Univ.

- ElAgami, N.L. ; Ibrahim, E.H., and Odah, H.H., 2000. Sedimentary origin of the Mn-Fe ore of Um Bogma, southwest Sinai: Geochemical and paleomagnetic evidence. *Econ. Geol.*, 95, 607-620.
- El Sharkawi, M.A. ; El-Aref, M., and Abdel Motelib, A., 1990. Manganese deposits in a Carboniferous paleokarst profile, Um Bogma region, West Central Sinai, Egypt. *Mineral. Depo.*, 25, 343p.
- El Shazly, E.M., and Saleeb, G.S., 1969. Contribution to the mineralogy of Egyptian manganese deposits. *Econ. Geol.*, 54, 873-888.
- El Shazly, E.M. ; Shukri, N.M., and Saleeb, G.S., 1963. Geological studies of OleikatMarahil and Um Sakran manganese-iron deposits, west central Sinai. *J. Geol., Egypt.*, 7, 1-27.
- Fitzgerald, C.E., and Gillis, K.M. 2006. Hydrothermal manganese oxide deposits from Baby Bare seamount in the Northeast Pacific Ocean. *Marine Geology*, 225, 145-156.
- Flinter, B.H., 1959. A magnetic separation of some alluvial minerals in Malaya. *American Mineralogist*, 44, No. 7-8, 738-751.
- Fryer, B.J., 1977. Rare earth evidence in iron formations for changing Precambrian oxidation states. *Geochimica et Cosmochimica Acta*, 41, 361-367.
- Gindy, A.R., 1961. On the radioactivity and origin of the manganese-iron deposits of west central Sinai. *Egyptian Academy Science*, 16, 71-86.
- Graf, W.L., 1977. The rate law in fluvial geomorphology. *Amer. J. Sci.*, 277, 178-191.
- Graselly, G.Y., and Hetengi, M., 1971. The role of manganese minerals in the migration of elements. *Special Issue Society Mining Geology Japan*, 3, 464-477.
- Gromet, L.P. ; Dymek, R.F.; Haskin, L.A., and Korteve, R.L. 1984. The "North American Shale Composite": Its compilation, major and trace element characteristics. *Geochim. Cosmochim. Acta*, 48, 2469-2482.
- Hansink, J.P., 1976. Equilibrium analysis of sandstone rollfront uranium deposits. *Proc. Inter. Symposium on exploration of uranium deposits. Int. Atomic Energy Agency, Vienna*, 683-693.
- Haskin, M.A., and Haskin, L.A., 1966. Rare earths in European shales: are determination. *Science*, 154, 507-509.
- Hein, J.R. ; Koschinsky, A.; Halbach, P.; Manheim, F.T.; Bau, M.; Kang, J.K., and Lubick, N., 1997. Iron and manganese oxide mineralization in the Pacific. In: *Manganese Mineralization; Geochemistry and mineralogy of terrestrial and marine deposits, Geological Society Special Publication 119*. Nicholson, K., Hein, J. R., Buhn, J. R. and Dasgupta, S. (Eds.). 123-138. Bath, U.K.: The Geological Society.
- Huawen, Q. ; Ruizhong, H., and Wenchao, S., 2002. REE geochemistry of Lignites in the Lincang-germanium deposit, Western Yunnan Province, China. *Goldschmidt Conference Abstracts*. 19.
- Jiangli, P., 1999a. Geochemical Behavior of Rare Earth Elements in Jianchaling Ore Deposit in Shaanxi Province. *J. Rare Earths*, 17:3.
- Jiangli, P., 1999b. Geochemistry of Rare Earth Elements in Hydrothermal Ore Deposit in Heishan Area, Shaanxi Province. *J. Rare Earths*, 17:1.
- Jiang, S.Y. ; Yu, J.M., and Lu, J.J., 2004. Trace and rare-earth element geochemistry in tourmaline and cassiterite from the Yunlong tin deposit, Yunnan, China: implication for migmatitic hydrothermal fluid evolution and ore genesis. *Chemical Geology*, 209, 193-213.
- Kato, Y., 1999. Rare Earth Elements as an Indicator to Origins of Skarn Deposits: Examples of the Kamioka Zn-Pb and Yoshiwara-Sannotake Cu (-Fe) Deposits in Japan. *Resource Geology*, 49(4), 183-198.
- Khalil, I.K., 1988. Comparative geological and mineralogical studies of manganese deposits of some localities in west central Sinai, A.R.E.M. *Sc. Thesis*, 192p.

- Kora, M., 1984. The Paleozoic exposures of Um Bogma area, Sinai. Ph. D Thesis, Fac. Scien. Mans. Univ., 280p.
- Magaritz, M., and Brenner, I.B., 1979. The geochemistry of a lenticular manganese ore deposits (Um Bogma, Southern, Sinai). *Mineralium-Deposita*, 14, 1-13.
- Mart, J., and Sass, E., 1972. Geology and origin of the manganese ore of Umm Bogma, Sinai. *Economic Geology*, 67, 145-155.
- McSween, H.Y., 1976. Manganese-rich ore assemblages from Franklin, New Jersey. *Economic Geology*, 71, 814-817.
- Mills, R.A., and Elderfield, H., 1995. Rare earth element geochemistry of hydrothermal deposits from the active TAG Mound, 26°N Mid-Atlantic Ridge. *Geochim. Cosmochim. Acta*, 59, 3511-3524.
- Nakhla, F.M., and Shehata, M.R., 1963. Mineralog-raphy of some manganese-iron ores from west central Sinai, Egypt. *Abhandlungen Neues Jahrbuch Mineralogie*, 99, 277-294.
- Nicholson, K., 1992. Contrasting mineralogical-geochemical signatures of manganese oxides: Guide to metallogenesis, *Economic Geology*, 87, 1253-1264.
- Quinif, Y.; Meon, H.; Yans, J., 2006. Nature and dating of karstic filling in the Hainaut Province (Belgium). *Karstic, geodynamic and paleogeographic implications. Geodinamica Acta.*, 19, 73-85.
- Roy, S., 1981. *Manganese deposits*. 457p. Academic Press Inc. London, Ltd.
- Saad, N.A.; Zidan, B.I., and Khalil, I.K., 1991. Manganese ore deposits of west central Sinai, Egypt: Its mineralogy and genesis. Second Geochemical Conference, Alexandria University, Egypt, 60-80.
- Saleeb-Roufai, G.S.; Yanni, N.N., and Amer, K.M., 1987. Contribution to the study of manganese-iron deposits at Umm Bogma area. Earth Science series, Ain Shams Univ., 1, 98-107.
- Sallam, O.R.; Alshami, A.S.; Mohamed, S.A., and El Akeed, I.A., 2014. The occurrence of silver-gold mineralization associated with uranium bearing minerals and base metal sulphide, El Sheikh Soliman Area, South Sinai, Egypt. *Egypt. J. Pure & Appl. Sci.*, 52(1), 47-54.
- Shapiro, L., and Branockis, W.W., 1962. Rapid analysis of silicate, carbonate and phosphate rocks. *U. S. Geol. Surv. Bull.*, 114A, 56.
- Shata, A.E., and El Balakassy, S.S., 2012. Supergene enrichments of uranium mineralization within Mn-Fe deposits of Um Bogma area, Southwest Sinai, Egypt. *Sedimentology of Egypt*, 20, 35-48.
- Soliman, S.M., 1961. Geology of the manganese deposits of Um Bogma, Sinai and its position in the African manganese production. 1st Iron and Steel Congress, 1-21.
- Smith, P.A., and Cronan, D.S., 1975. The dispersion of metals associated with an active submarine exhalative deposit. *Proc. 3rd oceanology international brighton conference England*, 111-114.
- Strakhov, N.M.; Zalmanzon, E.S.; Belova, I.V.; Dvorotskaya, D.A.; Lubchenko, Y.I.; Motuzova, G.V., and Cherkasova, E.V., 1967. Minor elements in the formations of sedimentary manganese ore. *Lithology mineral resources*, 3, 279-302.
- Taylor, S.R., and McLennan, S.M., 1981. The composition and evolution of the continental-crust-rare-earth element evidence from sedimentary-rocks. *Philosophical transactions of the Royal Society of London* 301(1461), 381-399.
- Toth, J.R., 1980. Deposition of submarine crusts rich in manganese and iron. *Geol. Soc. America Bul.*, Pt. 1(91), 44-54.
- Usui, T.; Wakatsuki, Y.; Matsunaga, Y.; Kaneko, S.; Koseki, H., and Kita, T., 1997. Over expression of B cell-specific activator protein (BSAP/Pax-5) in a late B cell is sufficient to suppress

- differentiation to an Ig high producer cell with plasma cell phenotype. *J. Immunol.*, 158, 3197-3204.
- Varnavas, S.P., 1979. Geochemical investigations on sediments from the Eastern Pacific. Ph.D. Thesis, University of London, 429.
- Varnavas, S.P., and Cronan, D.S., 1981. Partition-geochemistry of sediments from DSDP 424 in the Galapagos hydrothermal mounds field. *Mineralogic Magazine*, 44, 325-331.
- Weissbrod, T., 1969. The Paleozoic outcrops in South Sinai and their correlation with those of southern Israel. In: *The Paleozoic of Israel and adjacent countries*. *Bull. Geol. Surv.*, 2, 17-32.

أصل خام الفيرومنجنيز الحامل للمعادن المشعة في منطقة ام بجمه، جنوب غرب سيناء، مصر

أسامه رياض محمد سلام

يتناول البحث دراسة أصل نشأة خام الفيرومنجنيز المشع ببعض المواقع بمنطقة ام بجمه جنوب غرب سيناء. العديد من الشواهد الحقلية تؤكد ان أصل النشأة هي المحاليل الحارة اهمها وجود الخام على شكل عدسى و على شكل قواطع افقيه و راسيه. من الناحية المعدنية ، وجود معدنى الكاولينيت و الهوسمانيت يؤكد على النشأة من المحاليل الحارة. كيميائيا، خام الفيرومنجنيز محل الدراسة غنى بعناصر الباريوم، الزنك، الخارصين، اليورانسيوم، الفانديوم و النحاس و فقير فى عناصر الماغنيسيوم، الصوديوم، البوتاسيوم، الكالسيوم و النيكل. كذلك يتميز الخام بانخفاض محتوى العناصر الارضية النادرة و ايضا نسبة العناصر الارضية النادرة الخفيفة اعلى من الثقيلة. كل هذه الخصائص الكيميائية تؤكد نشأة الخام من المحاليل الحارة. يحتوى الخام على بعض معادن اليورانسيوم و الثوريوم مثل السايريت، الثوريت و اليورانوثوريت.